

# Fracture Mechanisms in Preformed Polyphenylene Oxide Particle-Modified Bismaleimide Resins

GUANGXUE WEI, H.-J. SUE

Polymer Technology Center, Department of Mechanical Engineering, Texas A&M University, College Station, Texas 77834-3123

Received 24 December 1998; accepted 12 May 1999

**ABSTRACT:** Fracture toughness and failure mechanisms in preformed poly(2,6-dimethyl-1,4-phenylene oxide) (PPO) particle-modified bismaleimide (BMI) systems are investigated. The fracture toughness of BMI can be significantly improved by incorporating preformed PPO particles without causing significant deterioration in other mechanical and thermal properties. The fracture mechanisms in BMI/PPO appear to be dominated by craze-like damage. Further investigation of the craze-like damage zone using transmission electron microscopy reveals that crazes are formed inside the PPO particle phase and dilatation bands, which appear to be triggered by the crazes inside the PPO particle, are formed in the BMI matrix. Particle bridging is also found to contribute to the toughening of BMI/PPO. The benefits of using preformed PPO particles to toughen BMI and other brittle thermosets for composite and adhesive applications are discussed. © 1999 John Wiley & Sons, Inc. *J Appl Polym Sci* 74: 2539–2545, 1999

**Key words:** rigid–rigid polymer toughening; fracture mechanism; dilatation band; high performance composite; preformed particle

## INTRODUCTION

Bismaleimide (BMI) resins are widely used as high performance composite matrices for their high temperature resistance, high glass transition temperature ( $T_g$ ), superior specific strength and specific modulus, and good epoxy-like processability. Unfortunately, BMI resins are brittle, which limits their structural applications. To enhance fracture toughness of BMI resins, several methods, such as chain extension with aromatic diamine through the Michael addition reaction<sup>1–3</sup> and by modification with reactive liquid rubbers,<sup>4,5</sup> were used. However, these methods cause undesirable reductions in modulus and glass transition temperature ( $T_g$ ). Significant research on BMI toughening is still needed.

More recently, ductile thermoplastics were utilized as tougheners to improve the fracture resistance of highly crosslinked thermoset resins. Most of the efforts in the literature involve the dissolution of thermoplastic particles in the thermosetting matrix, followed by precipitation of thermoplastic particles.<sup>6–9</sup> This type of approach usually does not render reproducible mechanical property unless the thermoplastic particle concentration is high. The recent research work of Pearson and Yee showed that poly(2,6-dimethyl-1,4-phenylene oxide) (PPO) particles can increase the fracture toughness of epoxy matrix by as much as 350%.<sup>10</sup> They attributed the toughening effect to the formation of multiple crack/microcracks in the damage zone.

To our knowledge, there is no known effort<sup>6</sup> focusing on using preformed thermoplastic particles to toughen BMI matrix. It is also not known what effective toughening mechanisms can operate in BMI resins. The present study intends to

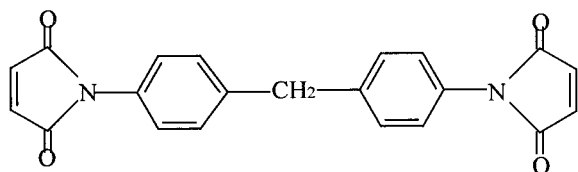
---

Correspondence to: H.-J. Sue.

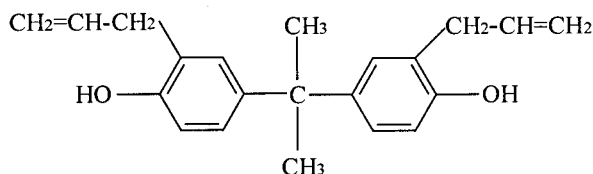
*Journal of Applied Polymer Science*, Vol. 74, 2539–2545 (1999)

© 1999 John Wiley & Sons, Inc.

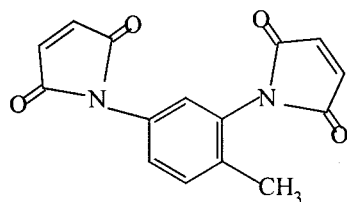
CCC 0021-8995/99/102539-07



4,4' - Bismaleimidodiphenylmethane (44 wt%)



0,0' - Diallyl Bisphenol A (32 wt%)



BMI-1, 3-tolyl (24 wt%)

**Figure 1** The structure of the three-component BMI.

investigate the effectiveness of using preformed PPO particles, as opposed to the utilization of soluble thermoplastic particles, to toughen brittle BMI. The advantages of using preformed thermoplastic particles to toughen thermosets are discussed.

## EXPERIMENTAL

All materials used in this investigation were received from commercial sources, and were used as received. The three component BMI (BMI-4,4'-MDA, BMI-1,3-tolyl, and o,o'-diallylbisphenol A), termed Cytec 5250-4-RTM BMI resin, was obtained from Cytec. The chemical structures of BMI are shown in Figure 1.

The PPO particles, in powder form, were received from General Electric Company. The PPO particles were sieved using U.S.A. Standard Testing Sieve (A.S.T.M.E-11 Specification) with 270 mesh. The particles with size less than 50  $\mu\text{m}$  were collected and utilized for toughening BMI.

The BMI resin is sticky at room temperature, and begins to melt at temperatures above 50°C. Upon heating to 100°C, the BMI resin exhibits low viscosity and can be easily processed. The PPO particles were gradually added at 100°C with continuous stirring for about 30 min to ensure good dispersion. Degassing was then carried out under vacuum at 120–130°C for about 1–3 h, depending on the PPO content in BMI. The resin was then cast into 5 × 4 × 1/8" (12.7 × 10.2 × 0.32 cm) plaques, using Teflon-coated metal plates, followed by curing for 6 h at 185°C and postcuring for 6 h at 220°C in an air-circulated oven. The oven was then turned off and slowly cooled to room temperature (25°C). The PPO particles, ranging from 5 to 20% by weight, were added to BMI. The finished plaque was machined into bars with dimensions of 6.35 × 1.27 × 0.32 cm for the double-notch four-point bend (DN-4PB)<sup>11–13</sup> experiment and the single edge-notch three-point bend (SEN-3PB) plane strain critical stress intensity factor ( $K_{IC}$ ) fracture toughness measurements.<sup>14,15</sup>

The dynamic mechanical behavior of the neat and thermoplastic-modified BMI resins was studied using dynamic mechanical spectroscopy (Rheometrics RMS-800) in a torsional mode, with 2.5°C per step. A constant strain amplitude of 0.1% and a fixed frequency of 1 Hz were used. The samples were tested at temperatures ranging from 25 to 380°C. Tan  $\delta$  peak was assigned as  $T_g$ .

The DN-4PB and SEN-3PB bars were notched with a 45° notching cutter (250  $\mu\text{m}$  crack-tip radius), followed by liquid nitrogen-chilled razor blade tapping to wedge open a sharp crack. The SEN-3PB method was utilized for fracture toughness measurements. The ratio of the crack length (a) to the specimen width (w) was chosen to be between 0.3 and 0.7 for the SEN-3PB test. A constant crosshead speed of 0.5 mm/min was chosen to conduct the SEN-3PB, three-point bend-flexural (3PB-F) test, and DN-4PB experiments. Care was taken to ensure that the upper contact loading points were touching the DN-4PB specimen simultaneously.

Optical microscopy (OM), scanning electron microscopy (SEM), and transmission electron microscopy (TEM) were used to study the fracture mechanisms in BMI blends. The detailed microscopy procedures for preparing the samples can be found elsewhere.<sup>11–13</sup>

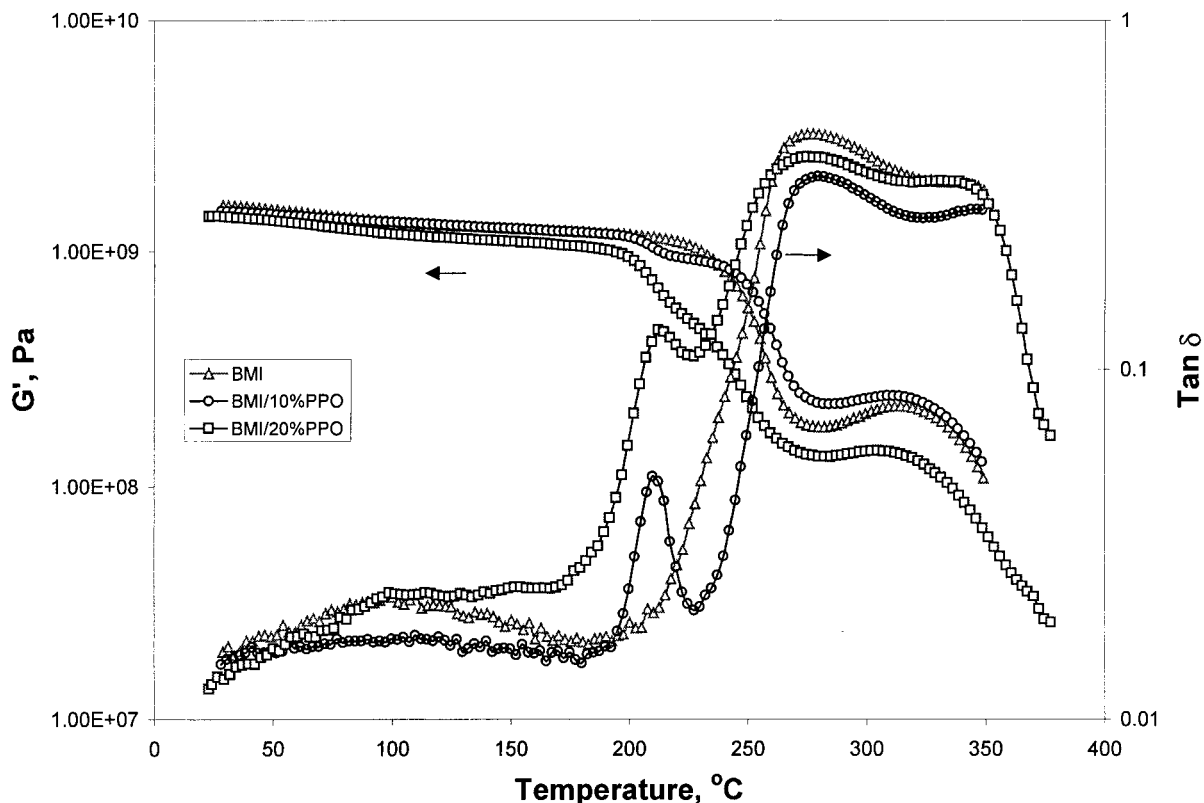


**Figure 2** Dynamic mechanical spectra of neat BMI vs. PPO-modified BMI resins.

## RESULTS AND DISCUSSION

### Dynamic Mechanical Analysis

The dynamic mechanical spectra of neat and modified BMI resins are given in Figure 2. The BMI resin has a  $T_g$  of 276°C. When 10 wt % PPO particles were used to toughen the BMI resin, the shear storage modulus begins to show a small drop above the  $T_g$  of PPO (210°C). The  $T_g$ , as well as the rubbery plateau modulus of the matrix, appear to be almost the same between the neat and PPO-modified BMI. On the other hand, when 20 wt % PPO was added to BMI resin, reductions in shear storage modulus ( $G'$ ) of the blend become significant when temperature is above 80°C. Also, the  $\tan \delta$  peak at  $T_g$  of the PPO particle phase is not completely separated from the  $\tan \delta$  peak of BMI at the  $T_g$  of BMI. This is probably due to the incomplete curing of BMI. It is also noted that the rubbery plateau moduli are very high for all three systems, which indicates the high crosslink density nature of BMI resins. The molecular weights between crosslinks calculated from rubbery plateau moduli range from 155 to 172 g/mol for the

three systems (Table I). Furthermore,  $G'$  of the matrix increases slightly and then decreases sharply after the temperature goes above  $T_g$  of the BMI matrix. The increase may be due to an incomplete curing of the BMI resin, as mentioned above. The sharp drop of  $G'$  with the temperature above  $T_g$  is probably due to devitrification and/or decomposition of BMI matrix.

### Mechanical Properties

The fracture toughness measurements of neat and modified BMI were conducted based on the linear elastic fracture mechanics approach (LEFM).<sup>16,17</sup> Flexural moduli were measured on an unnotched specimen according to ASTM D790. The mechanical property values reported are based on an average of at least five tests. The results are shown in Table I.

The  $K_{IC}$  of the neat resin was found to be about 0.87 MPa-m<sup>1/2</sup>, indicating that the BMI resin is not very brittle when compared with the one and two component BMI systems.<sup>4,5,18</sup> All of the PPO-modified samples displayed increases in  $K_{IC}$  values over that of the neat BMI resin. The higher

**Table I** The Selected Properties of BMI/PPO Systems

Materials	$K_{IC}$ (MPa·m <sup>1/2</sup> )	$G_{IC}$ (J/m <sup>2</sup> )	$E_f$ (GPa) <sup>a</sup>	$G'$ (MPa) <sup>b</sup>	$Mc$ g/mol	$T_g$ (°C) <sup>c</sup>
Pure BMI	0.87 ± 0.03	160	4.21	180	162	276
BMI/5%PPO	1.05 ± 0.11	—	—	—	—	—
BMI/10%PPO	1.26 ± 0.05	350	3.96	226	156	279
BMI/15%PPO	1.32 ± 0.04	390	3.92	—	—	—
BMI/20%PPO	1.40 ± 0.03	445	3.87	135	172	275

<sup>a</sup> Flexural modulus.<sup>b</sup> Rubbery shear storage modulus.<sup>c</sup> Temperature at which tan  $\delta$  curve at freq. = 1 Hz is a max.

PPO content appears to give greater improvement in  $K_{IC}$  (Fig. 3). However, when the PPO content is above 10 wt %, the toughening effect appears to be dropping off. Flexural moduli of neat and PPO-modified BMI at room temperature are also shown in Table I. The modulus shows a decrease from 4.21 GPa for neat BMI to 3.87 GPa for the BMI/20% PPO blend. The addition of thermoplastic particles did not affect the  $T_g$  of BMI.

### Fracture Mechanisms Investigation

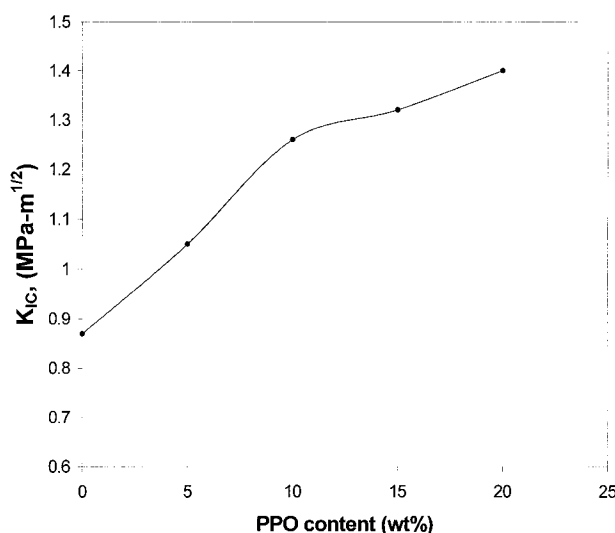
It is generally recognized that successful toughening in highly crosslinked thermosetting materials can be achieved by introducing energy dissipation processes that do not depend on matrix ductility. The work of Sue and Yee<sup>19</sup> indicated that if the inclusion (toughener) phase can initiate crazes upon fracture, it is possible to extend

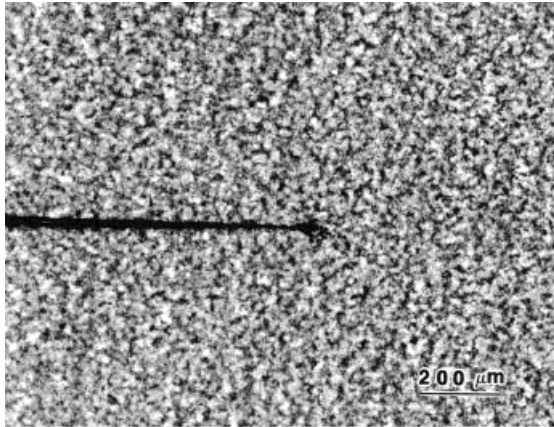
these crazes into the matrix phase as long as the matrix is prone to crazing. With this idea in mind, the craze-prone PPO particles are utilized to toughen BMI resin. It is anticipated that the PPO particles can trigger dilatation bands in this highly crosslinked BMI matrix.<sup>20,21</sup>

To study the fracture mechanisms, the sub-critically propagated crack of a DN-4PB specimen is analyzed using TOM. As shown in Figure 4, it is evident that a small cavitation zone is formed at the crack tip region [Fig. 4(a)]. When the damage zone is viewed under cross-polars, a large highly symmetrical birefringent zone [Fig. 4(b)] is observed. This birefringent zone is formed mainly due to the residual stress field, which makes it very difficult to definitively identify the extent of the crack tip plastic deformation, if any. To unambiguously determine the possible damage mechanisms in the crack tip damage zone, TEM investigation is undertaken.

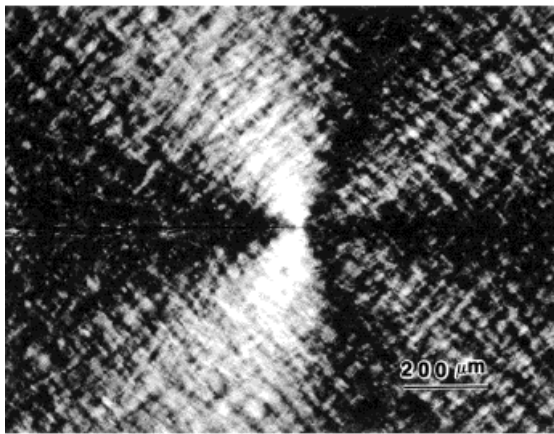
When the DN-4PB damage zone is observed using TEM, it is evident that crazes are formed inside the PPO particle (Fig. 5). Crack blunting behind the PPO particle is also observed (Fig. 6). These fracture energy dissipation processes prevent or slow down the crack from further propagation. The crazes are limited to inside the PPO particle and do not extend into the matrix.

Further investigations of the damage zone by TEM, as shown in Figures 7 and 8, indicate that dilatation bands associated with PPO particles were generated near the crack tip. This type of dilatation band was also observed in other thermosetting resins.<sup>20,21</sup> When the crack continues to grow, the dilatation bands are eventually broken into cracks at both sides of the particle (Fig. 7). These particles bridge the cracks, which slows down crack propagation. As pointed out by Bucknall,<sup>22,23</sup> rubber particles in craze-prone plastics

**Figure 3** Effects of PPO content on  $K_{IC}$  of BMI/PPO blends.



(a)



(b)

**Figure 4** Transmitted optical micrographs of BMI/10%PPO taken at the crack tip of a DN-4PB specimen, viewed under (a) bright field and (b) cross-polarized light. The crack propagates from left to right.

have two separate functions that are to initiate and terminate crazes. The termination of crazes can prevent crazes from growing into the cracks. The same roles are observed for PPO particles in BMI (Fig. 8). PPO particles as small as  $1\ \mu\text{m}$  in diameter can still generate massive dilatation bands (Fig. 8). It is somewhat surprising to observe dilatation bands in such a highly cross-linked thermoset system. It is possible that heterogeneous crosslinking took place in the BMI matrix, which allows the less crosslinked region to form dilatation bands.

It is often reported that in highly crosslinked thermoset systems, the primary fracture mechanisms are particle bridging instead of shear banding or crazing. To verify whether or not crack bridging is also a key toughening mechanism in the BMI/PPO system, SEM observation on frac-

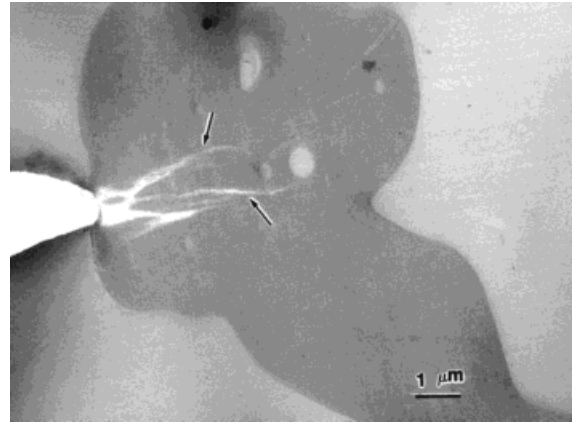


**Figure 5** TEM micrograph of BMI/10%PPO taken at the crack tip damage zone of the DN-4PB specimen. Crazes inside the PPO particle are evident at the crack tip (see arrow). The crack propagates from left to right.

ture surface was conducted. Figure 9 shows the fracture surface of the 10 wt % PPO-modified BMI resin. Addition of PPO particles leads to the formation of two distinct phases. The size and shape of the PPO particles remain almost the same as the original ones, which indicates that the PPO particle and BMI are totally immiscible. It is noted in Figure 9 that the crack goes through the PPO particles, and every PPO particle on the fracture surface is deformed and shows ductile drawing, which is a sign of crack bridging. However, the level of particle stretching is found to be insignificant. Therefore, the contribution of particle bridging in PPO-modified BMI is likely to be insignificant. On the other hand, the massive

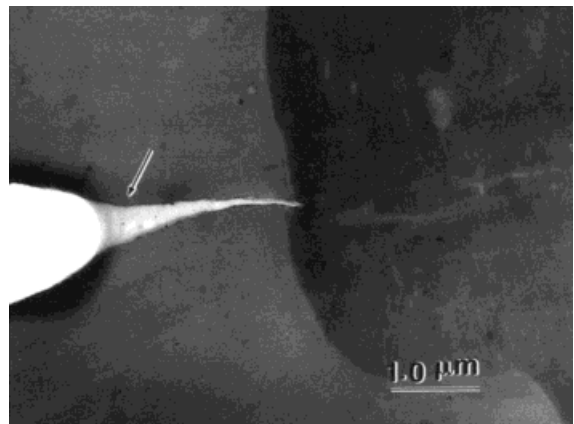


**Figure 6** TEM micrograph of BMI/10%PPO taken at the crack tip damage zone of the DN-4PB specimen. Crack blunting is observed (see arrow). The crack propagates from left to right.

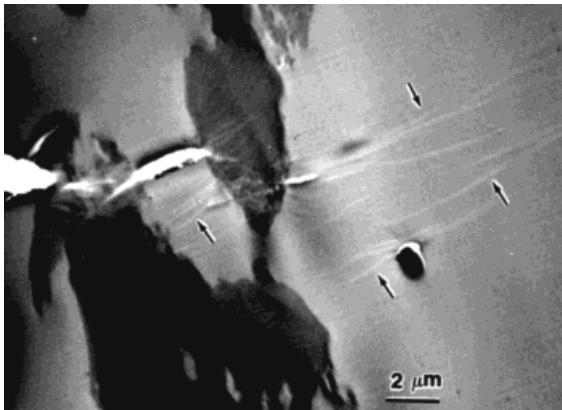


**Figure 7** TEM micrograph of BMI/10%PPO taken around the crack tip damage zone of the DN-4PB specimen. Dilatation bands (see arrows) are observed around the crack tip. The crack propagates from left to right.

crazes found inside the PPO particles could absorb a significant amount of fracture energy (Fig. 10). It is interesting to note that the interfacial adhesion between PPO particles and BMI matrix is very good. No particle-matrix debonding is found in both SEM and TEM observations. The probable reason may be due to mechanical interlocking at the interface during curing. The presence of strong interfacial adhesion is important for particle-induced matrix deformation in a highly crosslinked system, which results in the promotion of massive dilatation bands in BMI matrix.

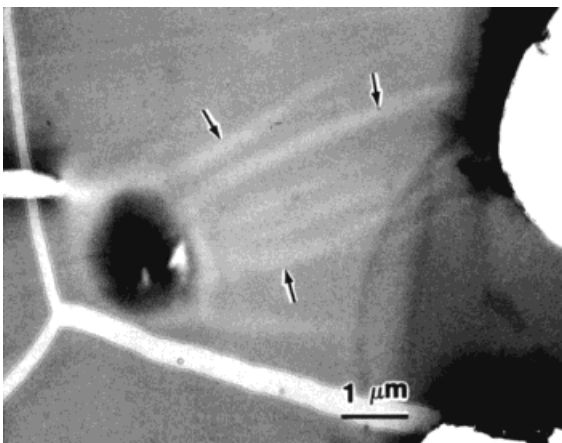


**Figure 8** TEM micrograph of BMI/10%PPO taken at the crack tip of the DN-4PB specimen. Dilatation bands (see arrows) induced by the PPO particle are observed. The crack propagates from left to right.

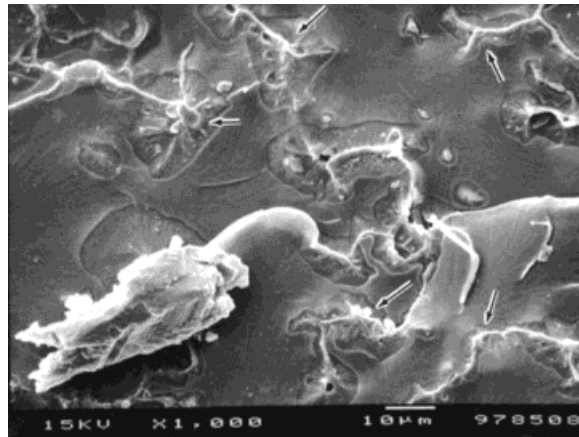


**Figure 9** SEM micrograph of the fracture surface of the BMI/10%PPO specimen. Particle drawing (see arrows) are observed.

Dilatation bands, crack tip blunting, and crack bridging are shown to operate in PPO-modified BMI. To probe whether or not dilatation bands and crack tip blunting exist in neat BMI specimens, a TEM study on the neat BMI DN-4PB damage zone was conducted. It was found that crack tip blunting does exist (Fig. 11), but when the crack opens further, catastrophic failure occurs. The crack-tip blunting mechanism just slows down crack propagation. In contrast to this behavior, if there is a PPO particle in front of the crack, the crack propagation can be blocked or slowed down by the presence of the PPO particle,

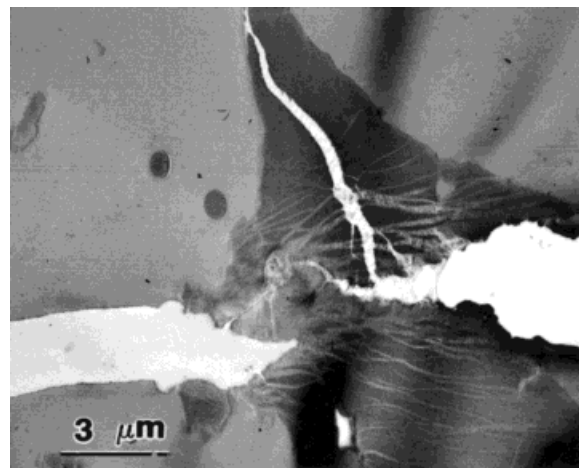


**Figure 10** TEM micrograph of BMI/10%PPO taken on the crack of the DN-4PB specimen. PPO particle drawing and massive crazes inside the PPO particle are observed. The crack propagates from left to right.

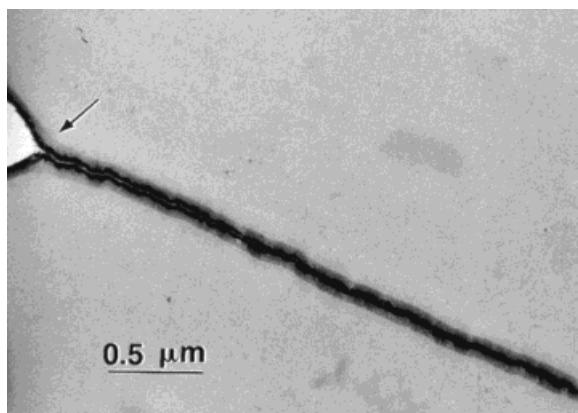


**Figure 11** TEM micrograph of the neat BMI specimen taken at the crack tip. Crack blunting is observed at the start of the crack tip (see arrow).

as shown in Figure 6. No dilatation bands were found in the neat BMI specimen.

## CONCLUSIONS

Ductile engineering thermoplastics such as PPO are shown to be effective modifiers for toughening brittle BMI. It is found that dilatation bands can form in the highly crosslinked PPO-modified BMI matrix. If suitable thermoplastic particles with appropriate size and concentration range were chosen, it is possible to generate massive dilatation bands in high performance thermosets. In turn, the toughness of the materials can be improved dramatically. The fracture mechanisms of BMI/PPO were mainly PPO particle crazing and dilatation band formation in the matrix.

## REFERENCES

1. Crivello, J. V. *J Polym Chem Ed* 1985, 11, 1973.
2. Verma, I. K.; Fohlen, G. M.; Parker, J. A. *J Polym Sci Polym Chem Ed* 1982, 20, 283.
3. Guilio, C. D.; Gautier, M.; Jasse, B. *J Appl Polym Sci* 1984, 29, 1771.
4. Takeda, S.; Kakiuchi, H. *J Appl Polym Sci* 1988, 35, 1351.
5. Abbate, m.; et al. *J Appl Polym Sci* 1997, 65, 979.
6. Rakutt, D.; Fitzer, E.; Stenzenberger, H. D. *High Perform Polym (UK)* 1991, 3, 59.
7. Bucknall, C. B.; Gilbert, A. H. *Polymer* 1989, 30, 213.
8. Kim, S. C.; Brown, H. R. *J Mater Sci* 1987, 22, 2589.
9. Kim, B. S.; Chiba, T.; Inoue, T. *Polymer* 1995, 36, 43.
10. Pearson, R. A.; Yee, A. F. *Polymer* 1993, 34, 3658.
11. Sue, H.-J.; Pearson, R. A.; Parker, D. S.; Huang, J.; Yee, A. F. *Polym Preprint* 1991, 29, 147.
12. Sue, H.-J. *Polym Eng Sci* 1991, 31, 270.
13. Sue, H.-J.; Yee, A. F. *J Mater Sci* 1989, 28, 2975.
14. ASTM Standard, D 5045-95.
15. Towers, O. L. *Stress Intensity Factor, Compliance and Elastic Factors for six Geometries*; The Welding Institute: Cambridge, UK, 1981.
16. Holik, A. S.; Kambour, R. P.; Hobbs, S. Y.; Fink, D. G. *Microstruct Sci* 1979, 7, 357.
17. Williams, G. *Fracture Mechanics of Polymers*; John Wiley & Sons: New York, 1984.
18. Iijima, T.; Hirano, M.; Fukuda, W.; Tomoi, M. *Eur Polym J* 1993, 29, 1399.
19. Sue, H.-J.; Yee, A. F. *J Mater Sci* 1989, 24, 1447.
20. Sue, H.-J.; Garcia-Meitin, E. I. *J Mater Sci Lett* 1993, 12, 1463.
21. Sue, H.-J.; Bertram, J. L.; Garcia-Meitin, E. I.; Puckett, P. M. *J Polym Sci B* 1995, 33, 2003.
22. Bucknall, C. B. *Toughened Plastics*; Applied Science Publishers Ltd.: London, 1977.
23. Bucknall, C. B. *Adv Polym Sci* 1978, 27, 121.